

## MAJOR PAPER

# Investigation of Acupuncture-specific BOLD Signal Changes Using Multiband Acquisition and Deconvolution Analysis

Tomokazu Murase<sup>1\*</sup>, Masahiro Umeda<sup>1</sup>, and Toshihiro Higuchi<sup>2</sup>

**Purpose:** We investigated the temporal dynamics of blood oxygen level-dependent (BOLD) signal responses during various stimuli, including real acupuncture, sham acupuncture, and palm scrubbing. For this purpose, deconvolution analysis was used to perform measurements using multi-band (MB) echo-planar imaging (EPI), which can improve time resolution, and to analyze brain responses without an expected reference function.

**Methods:** We divided 26 healthy right-handed adults into a group of 13 who received real acupuncture stimulation with manual manipulation and the other group of 13 who received sham acupuncture and palm scrubbing tactical stimulations. Data analysis was performed with a combination of analysis packages.

**Results:** We found stimulus-specific impulse responses of the BOLD signal in various brain regions. During real acupuncture, activated areas were observed in the secondary somatosensory cortex (SII) and insula during stimulation and in the anterior cingulate cortex (ACC), supplementary motor area (SMA), and thalamus after the stimulation. During sham acupuncture, activated areas were observed in the SII, insula, and thalamus during stimulation. During the scrubbing condition, activated areas were observed in the contralateral primary somatosensory cortex (SI), SII, insula, and thalamus during stimulation. In particular, during the real acupuncture condition, significantly delayed and long-sustained increased signals were observed in several brain regions, in contrast to the signals induced with sham acupuncture and palm scrubbing.

**Conclusion:** We speculated that the delayed and long-sustained signal increases were caused by peripheral nociceptors, flare responses, and time-consuming processing in the central nervous system. We used deconvolution analysis with MB EPI and tent functions to identify the delayed increase in the BOLD signal in the area related to pain perception specifically observed in real acupuncture stimulation. We propose that the specific BOLD signal change observed in this study will lead to the elucidation of the mechanism underlying the therapeutic effect of acupuncture stimulation.

**Keywords:** *acupuncture, multi-band echo-planar imaging, functional magnetic resonance imaging*

## Introduction

For longer than 2000 years, acupuncture has been used worldwide to treat various diseases and symptoms. However, the mechanism and effectiveness of acupuncture

remain to be elucidated. Functional MRI (fMRI) studies on acupuncture have typically been performed using block designs and analyzed using a general linear model (GLM). However, in GLM analysis using acupuncture stimulation timing, since the activation area is narrow, recent studies have called into question the equivalence of stimulation and sensation in block-design acupuncture experiments.<sup>1,2</sup> Furthermore, a previous study showed that prolonging of the needling sensation, introduced by acupuncture needling, could occur.<sup>3</sup> We previously reported that manual acupuncture triggers a characteristic temporal signal change that increases delay and long-lasting blood oxygen level-dependent (BOLD) signals using tent functional deconvolution analysis.<sup>4</sup> Since this characteristic temporal signal change may indicate acupuncture stimulation differing from other somatosensory stimuli, it is necessary to investigate the changes in the time-varying signal in more detail.

<sup>1</sup>Department of Medical Informatics, Meiji University of Integrative Medicine, Nantan, Kyoto, Japan

<sup>2</sup>Department of Neurosurgery, Meiji University of Integrative Medicine, Nantan, Kyoto, Japan

\*Corresponding author: Department of Medical Informatics, Meiji University of Integrative Medicine, 6-1, Hinotani, Honoda, Hiyoshicho, Nantan, Kyoto 629-0392, Japan. Phone: +81 -771-72-9000, Fax: +81 -771-72-1221, E-mail: murase@meiji-u.ac.jp



This work is licensed under a Creative Commons Attribution-NonCommercial-NoDerivatives International License.

©2021 Japanese Society for Magnetic Resonance in Medicine

Received: April 3, 2019 | Accepted: December 12, 2020

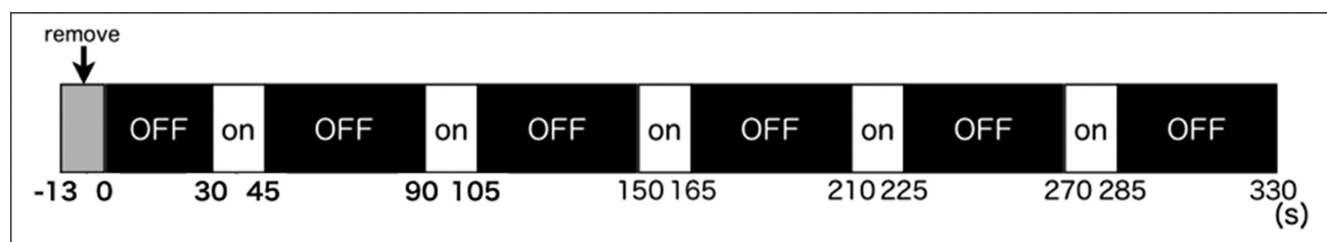


**Fig. 1** All fMRI run sequences consisted of five 15-s stimulation blocks (ON) that were interspersed between one 43-s and five 45-s rest blocks (OFF) for a total scanning time of 343 s. The first 13 data points from each dataset were discarded to ensure that the analyzed data were acquired from the stable state. fMRI, functional MRI.

Recent advances in multi-band (MB) echo-planar imaging (EPI) have enabled acquiring fMRI data with higher spatial and temporal resolutions. MB-EPI, which can accelerate the acquisition's temporal resolution to excite multiple slices simultaneously,<sup>5</sup> has therefore recently become a popular acquisition modality for fMRI. In this study, we used MB-EPI and deconvolution analysis to examine precisely signal changes in brain activity caused by acupuncture stimulation.

## Materials and Methods

Twenty-six healthy, right-handed adults (16 men and 10 women) aged 18 to 33 years provided written informed consent to participate in this study, which was approved by the Ethics Committee of Meiji University of Integrative Medicine. The 26 subjects were divided into two groups, with one group receiving real acupuncture stimulation with manual manipulation and the other receiving both sham acupuncture and scrubbing stimulations as control.

The right acupuncture point Hegu (LI-4), which is located on the dorsum of the right hand radial to the mid-point of the second metacarpal bone, was selected for the acupuncture stimulation site. The real acupuncture stimulation consisted of the following two steps. First, a non-magnetic silver needle (0.20 mm in diameter, 39-mm long; Asahi Iryouki, Saitama, Japan) was inserted into LI-4 to a depth of approximately 15 mm before beginning the fMRI scan run. Then, it was subsequently manually rotated bidirectionally approximately 180° at 1 Hz. Two types of tactile stimulation were used as controls: tapping with a von Frey monofilament (sham acupuncture) and scrubbing with a scrubbing sponge. Sham stimulation has been used as a tactile stimulus in the previous studies of fMRI,<sup>6</sup> and a scrubbing sponge has been used as a simple somatosensory stimulus.<sup>7</sup> Sham acupuncture was delivered to the skin surface at LI-4 by gentle tapping with a 5.88 von Frey monofilament. During the stimulation block, tapping was continuously applied at approximately 4 Hz. Another control stimulation was administered by scrubbing the subject's right palm with a scrubbing sponge in one direction at approximately 4 Hz. All acupuncture and tactile

stimulations were performed by a single licensed and experienced acupuncturist. All fMRI run sequences consisted of five 15-s stimulation blocks (ON) that were interspersed between one 43-s and five 45-s rest blocks (OFF) for a total scanning time of 343 s (Fig. 1).

Subjects were in the supine position and wearing ear-plugs while in the scanner. In order to minimize head motion, soft foam padding was inserted into the 32-channel head coil. fMRI scanning was conducted on a 3-T MAGNETOM Trio, A Tim System (SIEMENS, Munich, Germany) MRI scanner. Anatomical images were acquired with 3D T1-weighted magnetization-prepared rapid acquisition with gradient echo TR, 1900 ms; TE, 2.52 ms; inversion time, 900 ms; fractional anisotropy [FA], 9°; FOV, 25 cm; 176 axial slices; slice thickness, 1.0 mm; matrix size, 256 × 256, sagittal). Axial BOLD MR images were acquired with a MB gradient-echo EPI sequence from Minnesota University<sup>5,8</sup> (TR, 1000 ms; TE, 30 ms; FA, 60°; MB factor, 2; iPAT factor, 2; FOV, 22.4 cm; 36 axial slices; slice thickness, 3.5 mm; matrix size, 64 × 64). Based on previous research, data analysis was performed with a combination of analysis packages, including SPM8 (<http://www.fil.ion.ucl.ac.uk/spm>, Department of Cognitive Neurology, London, UK), MarsBaR (<http://marsbar.sourceforge.net>),<sup>9</sup> and the Analysis of Functional NeuroImages (AFNI) software program (<http://afni.nimh.nih.gov/afni/>).<sup>10</sup> Preprocessing was performed in the same manner as that reported in the previous research.<sup>4</sup> All functional images were aligned to the first volume, and the 3D anatomical images were then c-registered with the first volume of the functional scan. The 3D T1-weighted volume was spatially normalized to the Montreal Neurological Institute T1-weighted MRI template. The same transformation parameters were applied to all functional volumes, which included 3D spatial smoothing with an 8-mm full-width at half-maximum Gaussian kernel. The first 13 data points from each dataset were discarded to ensure that the analyzed data were acquired in the stable state. For statistical analysis, 3dDeconvolve, which is part of the AFNI package, was used to extract the impulse response functions (IRFs) of the fMRI signals on a voxel-wise basis. First, we assumed that 60 TRs, which included 15 TR periods for stimulation, were sufficient for extracting the IRFs. Then, the 31 tent basis

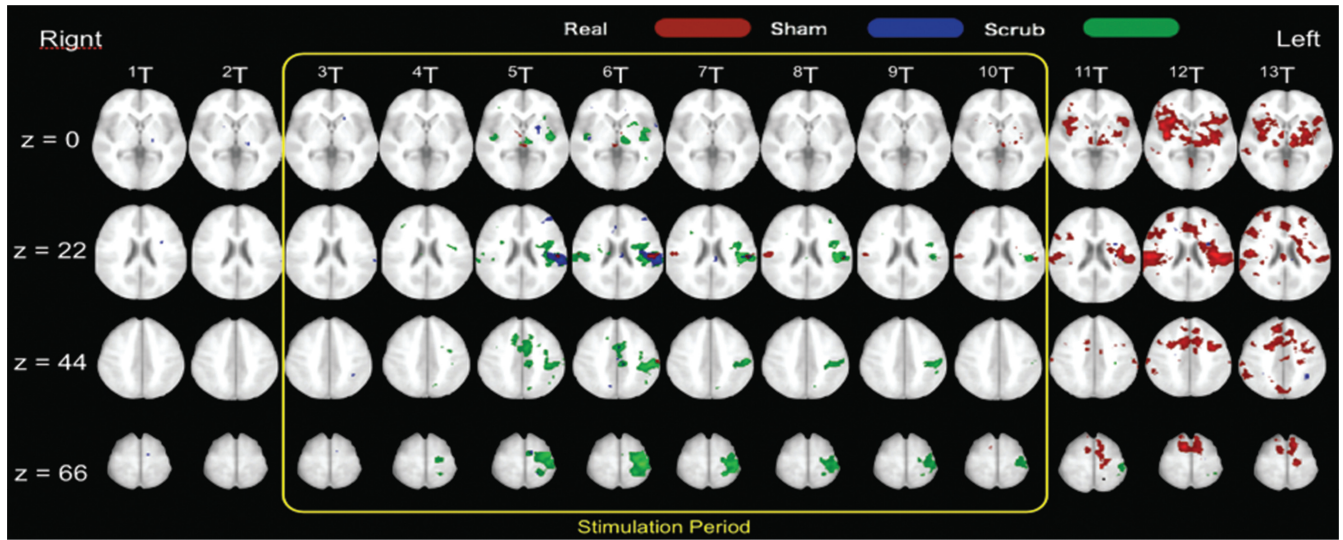


**Fig. 2** Overlapped group statistical maps for each tent function in the three groups ( $z = 0, 22, 44,$  and  $66$ ). Regions exhibiting significant activation during real acupuncture (red:  $N = 13$ ), sham acupuncture (blue:  $N = 13$ ), and the scrubbing (green:  $N = 13$ ). A random analysis was performed, and activations overlapped onto an axial slice of a standard brain ( $P < 0.001$ , uncorrected).  $^1T$ – $^{13}T$  indicate the temporal axis, and each interval of  $T$  represents  $2\text{ s}$  ( $= 2\text{ TR}$ ).  $T$ , tent function.

functions ( $^1T$ – $^{31}T$ ) covering 4 to 56 TRs (relative to the stimulus onset) were used to estimate the fitting coefficient (beta estimate). In this study, the  $^3T$ – $^{10}T$  functions corresponded to the actual stimulation period, and the 31 beta estimates were estimated for IRF extraction.<sup>11,12</sup> In order to eliminate the variance in each condition of interest across subjects, a random-effects analysis was performed using a one-sample  $t$ -test at each voxel across subjects based on their individual beta maps ( $P < 0.001$ , uncorrected) and clusters with a threshold size of over 10 voxels were then superimposed on high-resolution anatomical images (Fig. 2). Further, to examine the IRF, a cubic region of interest was defined using a set of voxels in a  $4 \times 4 \times 4\text{ mm}^3$  portion centered at the maximum  $t$  value for the area of activation cluster within each Brodmann area. Finally, the extracted IRF time course was calculated as the difference between the first time point's IRF and the IRF of each of the following time points, and then one sample  $t$ -test analysis at each time point.

## Results

Figure 2 shows the activated areas and temporal evolution of the brain responses during each stimulus. These data were consistent with the IRFs from the deconvolution analysis. During real acupuncture, areas of stimulus-induced activation were observed on both sides in the secondary somatosensory cortex (SII) and the insula in  $^5T$ – $^{10}T$  and on both sides in the anterior cingulate cortex (ACC), the supplementary motor area (SMA), and the thalamus after  $^{11}T$  (Fig. 2, red). In later phases, activation was also observed in the contralateral primary somatosensory cortex (SI) (data not shown). Results from the

fMRI performed during sham acupuncture showed activation in the contralateral SI, SII, SMA, the insula, and the thalamus during stimulation ( $^5T$ – $^8T$ ) (Fig. 2, blue). During the scrubbing condition, activated areas were observed in the contralateral SI, SII, insula, and thalamus during stimulation ( $^5T$ – $^{10}T$ ) (Fig. 2, green). These results demonstrated many similarities in activation between the sham acupuncture and scrubbing stimulation conditions. In contrast, real acupuncture induced more widespread brain activity and more delayed and long-sustained brain activity than the tactile stimulations did.

Figure 3 shows stimulus-dependent changes in IRF extracted from various brain regions. In SII, the insula, and the thalamus, we observed significant increases in BOLD signal amplitude during any stimulation type. These increases in amplitude peaked about 6 seconds after the start of stimulation and then declined. For real acupuncture stimulation only, the amplitude increased again after the end of the stimulation to a maximum peak around 5 seconds after the end of stimulation, and decreased thereafter. In the thalamus, this decrease was gradual, and was followed by another significant increase in amplitude 45 seconds after the end of stimulation. In the S1, the amplitude increased during the stimulation period with scrub and sham acupuncture stimuli. This peaked around 6 seconds into the stimulation period, followed by a decrease in amplitude. In contrast, with real acupuncture stimulation, we observed a significant increase in amplitude 15 seconds after the end of stimulation. This lasted 10 seconds before decreasing. In the SMA, we observed a significant increase in amplitude with scrub stimuli only during the stimulation period. Here, the amplitude peaked around 4 seconds after the start of stimulation and then decreased. With real acupuncture

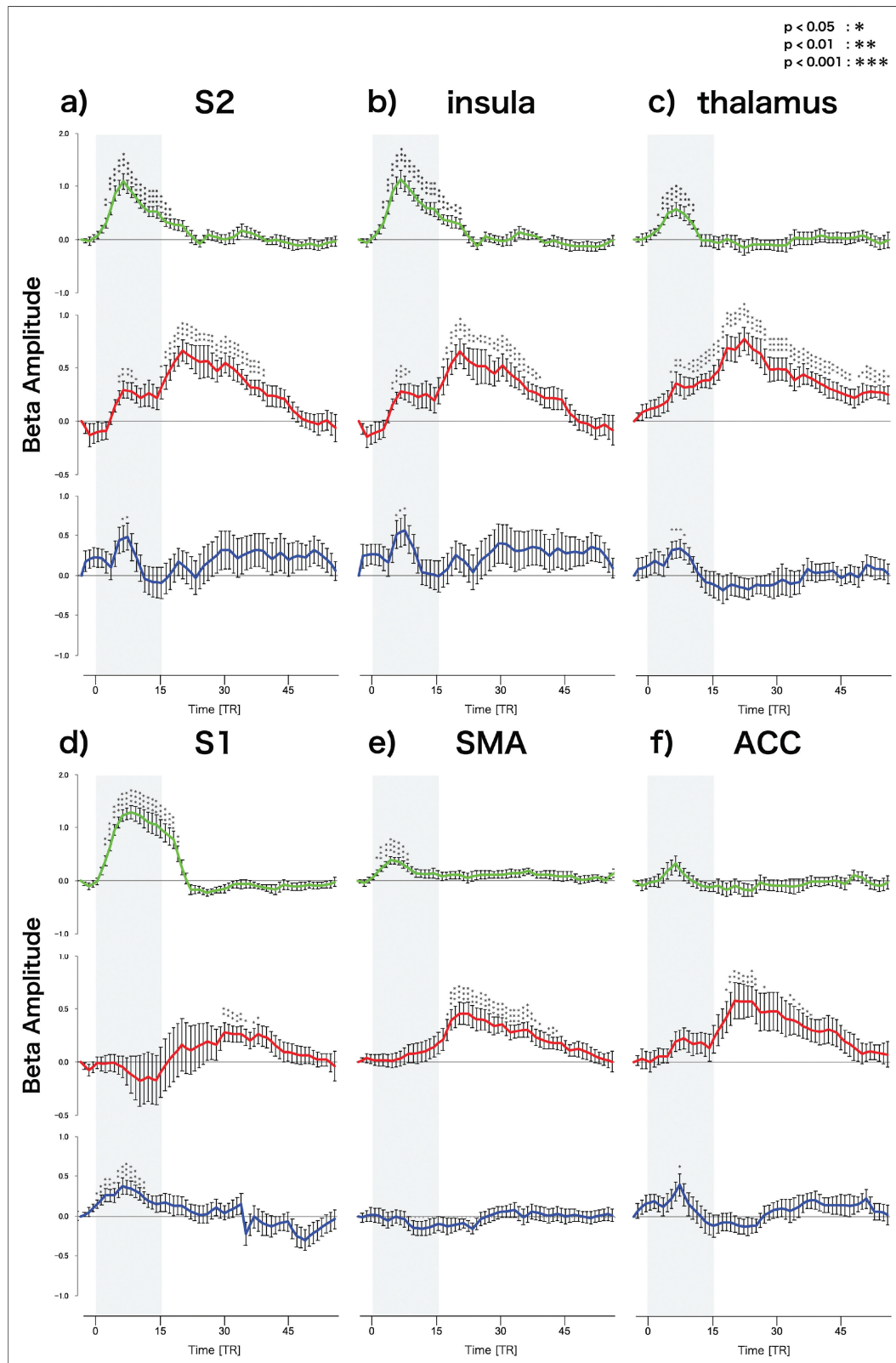


**Fig. 3** Time-course of the beta amplitude changes (means  $\pm$  SE) for real acupuncture (red), sham acupuncture (blue), and scrubbing (green) in the following regions: **a)** SII, **b)** insula, **c)** thalamus, **d)** SI, **e)** SMA, and **f)** ACC. The gray line indicates the stimulation period. Significant differences by region and at each TR are indicated. (\* $P < 0.01$ , \*\* $P < 0.005$ , \*\*\* $P < 0.001$ ). ACC, anterior cingulate cortex; SE, standard error; SI, primary somatosensory cortex; SII, secondary somatosensory cortex; SMA, supplementary motor area.

stimulation, the amplitude increased both during and after the stimulation period, reached a peak around 5 seconds after the stimulation end, and then decreased. In the ACC, we observed an increase in amplitude during the stimulation period under all stimulation conditions, but only sham stimulation showed a significant increase. However, with real acupuncture stimulation, we observed a significant increase in amplitude 30 seconds after the end of the stimulation, which lasted about 10 seconds before decreasing.

## Discussion

In this study, we investigated the temporal dynamics of BOLD signal responses during various stimuli, including real acupuncture, sham acupuncture, and palm scrubbing. In our previous work, the measurement environment was a 1.5T MRI machine (Signa; GE Healthcare, Waukesha, WI, USA) and a 1-ch standard head coil with a time resolution of 3 seconds, which was not enough to discuss dynamic changes in detail. To achieve a more suitable time resolution for observing dynamic changes in this study, we verified the multi-band EPI (which can improve time resolution) to increase the time resolution by a factor of three. We found stimulus-specific impulse responses of the BOLD signal in various brain regions. With real acupuncture stimulation, we observed a bimodal change with a signal increase both during and after stimulation.

We found that scrubbing stimulation was associated with more prominent activation of the sensorimotor brain regions (SI, SII, insula and SMA) during stimulation compared to those associated with real acupuncture and sham acupuncture. In addition, the IRF of palm scrubbing in these areas increased in signal at the start of stimulation and declined after the end of stimulation in all areas where activation was observed. Although we observed similar changes in BOLD signal amplitude in the SI, SII, the insula, and the thalamus with sham acupuncture stimulation, we noted differences in activation of the SMA and ACC. The function of the SMA relates to preparing for spontaneous movement, and for this area, we found BOLD signal amplitude increases when scrubbing the palm. The activation of SMA was considered to have been activated by the movement of fingers by scrubbing stimulus.<sup>4</sup> The function of the ACC relates to cognitive processing (such as experiencing pain). Since the acupoint has a low pressure-pain threshold,<sup>13</sup> this control stimulus may activate some of the pain-related areas in the ACC.

Conversely, with real acupuncture stimulation, we observed a bimodal change with an increase in BOLD signal amplitude both during and after stimulation. Signal elevation immediately after stimulation is considered a common to reaction somatosensory stimuli, but persistent signal elevation is considered a specific reaction to acupuncture stimulation. It has been suggested that the peripheral receptors involved in acupuncture stimulation are polymorphic C-fiber nociceptors.<sup>14</sup> As previously reported, manual acupuncture stimulation activates C fibers by releasing chemical substances resulting from deep

tissue injury.<sup>15</sup> In animal experiments on heat pain, a time lag until the threshold temperature of heat pain was reached that also delayed brain activity associated with noxious stimuli.<sup>16</sup> The acupuncture technique performed this time may have been somatosensory stimulation only for a short time, but it may be input as a noxious stimulus by continuing for a certain period of time. C-fiber activation is associated with the induction of a local reaction (flare reaction) by acupuncture stimulation.<sup>17,18</sup> Neurogenic inflammation induces local hyperalgesia. Furthermore, repeated C fiber input causes a reaction called windup increase after C fiber stimulation, which is considered to strengthen the input over time.<sup>19</sup> Because C fiber input does not stop immediately after the end of stimulation, it is considered that delay in signal change and long sustained signal increase will occur. The specific reaction induced by acupuncture stimulation is termed “de-qi”.<sup>20,21</sup> The sense of “de-qi” reportedly includes tingling and heaviness and numbness, and the perception of sensation induced by acupuncture stimulation is associated with time-consuming complicated processing in the central nervous system. Furthermore, fMRI in animal experiments has been reported to be affected by stimulation-induced changes in systemic physiological parameters, thus delaying signal increase due to electrical stimulation by approximately 10 seconds under medetomidine and urethane anesthesia.<sup>21</sup> Acupuncture stimulation has been reported to modulate the autonomic nervous system,<sup>22</sup> and delay in signal increase may indicate the effectiveness of acupuncture.

## Conclusion

The bimodal signal changes in brain activity were observed by acupuncture stimulation in this study; one occurred in common with somatosensory stimulation immediately after stimulation, and the other after the end of stimulation only real acupuncture stimulation. We suggest that the delayed and long-sustained signal increases were caused by peripheral nociceptors, flare responses, hemorrhagic changes caused by acupuncture and processing in the central nervous system.

We used deconvolution analysis with MB EPI and tent functions to identify the delayed increase in the BOLD signal in the area related to pain perception specifically observed in only real acupuncture stimulation. We propose that the specific BOLD signal change observed in this study will lead to the elucidation of the mechanism underlying the therapeutic effect of acupuncture stimulation.

## Acknowledgment

This work was supported by JSPS KAKENHI Grant Numbers JP15K19196, JP17K10910, JP18K08982.

## Conflicts of Interest

The authors declare that they have no conflict of interest.

## References

1. Ho TJ, Duann JR, Chen CM, et al. Carryover effects alter fMRI statistical analysis in an acupuncture study. *Am J Chin Med* 2008; 36:55–70.
2. Bai L, Qin W, Tian J, et al. Time-varied characteristics of acupuncture effects in fMRI studies. *Hum Brain Mapp* 2009; 30:3445–3460.
3. Ho TJ, Duann JR, Shen WC, et al. Needling sensation: explanation of incongruent conclusion drawn from acupuncture fMRI study. *J Altern Complement Med* 2007; 13:13–14.
4. Murase T, Umeda M, Fukunaga M, et al. Deconvolution analyses with tent functions reveal delayed and long-sustained increases of BOLD signals with acupuncture stimulation. *Magn Reson Med Sci* 2013; 12:121–127.
5. Moeller S, Yacoub E, Olman CA, et al. Multiband multislice GE-EPI at 7 tesla, with 16-fold acceleration using partial parallel imaging with application to high spatial and temporal whole-brain fMRI. *Magn Reson Med* 2010; 63:1144–1153.
6. Sun J, Qin W, Jin L, et al. Impact of global normalization in fMRI acupuncture studies. *Evid Based Complement Alternat Med* 2012; 2012:467061.
7. Fukunaga M, Tanaka C, Umeda M, et al. [Three-dimensional brain mapping using fMRI]. *No To Shinkei* 1997; 49:905–913. (in Japanese)
8. Setsompop K, Gagoski BA, Polimeni JR, et al. Blipped-controlled aliasing in parallel imaging for simultaneous multislice echo planar imaging with reduced g-factor penalty. *Magn Reson Med* 2012; 67:1210–1224.
9. Brett M, Anton JL, Valabregue R, et al. Region of interest analysis using an SPM toolbox. *NeuroImage*. 2002; 16:497.
10. Cox RW. AFNI: software for analysis and visualization of functional magnetic resonance neuroimages. *Comput Biomed Res* 1996; 29:162–173.
11. Cabeza R, Rao SM, Wagner AD, et al. Can medial temporal lobe regions distinguish true from false? An event-related functional MRI study of veridical and illusory recognition memory. *Proc Natl Acad Sci U S A* 2001; 98:4805–4810.
12. Saad ZS, Chen G, Reynolds RC, et al. Functional imaging analysis contest (FIAC) analysis according to AFNI and SUMA. *Hum Brain Mapp* 2006; 27:417–424.
13. Ben H, Li L, Rong PJ, et al. Observation of pain-sensitive points along the meridians in patients with gastric ulcer or gastritis. *Evid Based Complement Alternat Med* 2012; 2012:130802.
14. Kawakita K, Gotoh K. Role of polymodal receptors in the acupuncture-mediated endogenous pain inhibitory systems. *Prog Brain Res* 1996; 113:507–523.
15. Zhao ZQ. Neural mechanism underlying acupuncture analgesia. *Prog Neurobiol* 2008; 85:355–375.
16. Bosshard SC, Stucker F, von Deuster C, et al. BOLD fMRI of C-Fiber mediated nociceptive processing in mouse brain in response to thermal stimulation of the forepaws. *PLoS One* 2015; 10:e0126513.
17. Handwerker HO, Forster C, Kirchhoff C. Discharge patterns of human C-fibers induced by itching and burning stimuli. *J Neurophysiol* 1991; 66:307–315.
18. Rukwied R, Dusch M, Schley M, et al. Nociceptor sensitization to mechanical and thermal stimuli in pig skin in vivo. *Eur J Pain* 2008; 12:242–250.
19. Li J, Simone DA, Larson AA. Windup leads to characteristics of central sensitization. *Pain* 1999; 79:75–82.
20. MacPherson H, Asghar A. Acupuncture needle sensations associated with De Qi: a classification based on experts' ratings. *J Altern Complement Med* 2006; 12:633–637.
21. Yang XY, Shi GX, Li QQ, et al. Characterization of deqi sensation and acupuncture effect. *Evid Based Complement Alternat Med* 2013; 2013:319734.
22. Li QQ, Shi GX, Xu Q, et al. Acupuncture effect and central autonomic regulation. *Evid Based Complement Alternat Med* 2013; 2013: 267959.